A New Combination Method of N-doped TiO₂ Nanoparticles Synthesis for Heavy Metal Ions Cr(VI) Photoreduction Applications

Diana Vanda Wellia [a,*], M. Rafli Habibillah [a], Atika Syafawi [a], Rizka Rahmadini [a], Rahmayeni [a], Nurul Pratiwi [b]

[a] Department of Chemistry, Faculty of Mathematics and Natural Sciences, Andalas University, Padang, Indonesia
[b] Department of Chemistry, Faculty of Science and Technology, Jambi University, Jambi, Indonesia

* Corresponding author: nandadiana@sci.unand.ac.id

Article Info

Abstract

Through a combination of biosynthesis and hydrothermal methods, N-doped TiO₂ photocatalyst has been successfully synthesized using various concentrations of ammonia as a nitrogen source, namely 10% w/w (NTO10), 20% w/w (NTO20), 35% w/w (NTO35), and 50% w/w (NTO50). The synthesis of TiO₂ was conducted using *Aloe vera* (L) Burm F. rind extract as a natural capping agent via the biosynthesis method, followed by a nitrogen doping process via the hydrothermal method. The X-ray Diffraction (XRD) analysis revealed that all phases were anatase. According to the results of the UV-Vis Diffuse Reflectance Spectroscopy (UV-Vis DRS) analysis using the Tauc-Plot method, all N-doped TiO₂ samples showed a decrease in the energy gap compared to the TO sample. This indicates that the doping of TiO₂ using nitrogen has been successfully doped into TiO₂. The photocatalytic activity of N-doped TiO₂ was evaluated for the photoreduction of the Cr(VI) model pollutant using a 24-watt LED lamp as a visible light source for 120 minutes. The results indicate that the NTO35 is the best-prepared N-doped TiO₂, which showed a reduced rate for the Cr (VI) model pollutant of 50.88%, or two times greater than that of undoped TiO₂.

1. Introduction

Environmental pollution in water, soil, and air has recently become a significant concern for the community and the government [1]. Water, as one of the essential substances supporting human life, has increased in demand since it has been continuously polluted by countless contaminants over the last century [2]. Mostly, the main sources of water contamination are caused by the rapid growth of the industrial sector, such as mining, leather, steel, pigments, textile, and electroplating industries [3, 4]. These industries can potentially produce large amounts of wastewater containing hazardous inorganic chemicals, like heavy metals [5].

Chromium (Cr) is an example of a heavy metal that poses the highest risk to aquatic ecosystems due to its toxicity, non-biodegradability, and high propensity for accumulation in living organisms [6]. Chromium can exist in different oxidation states, such as Cr (VI) and Cr (III) [7]. Cr(III) is relatively less mobile, less toxic, and can easily be found in trace amounts as an essential nutrient in various biological pathways [8]. On the other hand, Cr(VI) is highly reactive, hazardous, and toxic. When Cr(VI) accumulates in the human body, it causes cancer, chronic ulcers, dermatitis, gastrointestinal system, as well as kidney and lung damage [9, 10]. Therefore, it is highly desirable to investigate appropriate methods for converting Cr(VI) to Cr(III) in contaminated wastewater.

Photocatalytic reduction is believed to be one of the most effective and efficient methods that are commonly used for converting Cr(VI) to Cr(III) by employing photocatalysts [11]. Among all the various photocatalysts, titanium dioxide (TiO₂) is often chosen due to its low cost, non-toxicity, outstanding physiochemical properties, and superior chemical stability [12]. As commonly known, TiO₂ nanoparticles can be synthesized using solvothermal, sol-gel, hydrothermal, and sonochemical methods [13, 14]. However, these methods frequently obtain nanoparticles with several shortcomings,

including a very high tendency to aggregate, an uneven distribution of particle size and shape, and the formation of nanoclusters [15]. Moreover, these methods also require complicated procedures and high costs due to the necessity for high pressure and energy [16].

Recently, nanoparticle biosynthesis methods have been widely used to overcome the limitations of conventional methods [17, 18]. Natural products, such as plant extracts containing biomolecules, have been intensively used as capping agents [19]. These natural biomolecules were mainly composed of polyphenols, which have been found to play an active role in the biosynthesis of nanoparticles from any plant extract capable of forming various shapes and sizes of nanoparticles with enhanced active surface area, characteristics and properties [16]. Therefore, biosynthesis can be considered the safe and environmentally friendly approach for many applications that have used TiO_2 nanoparticles [20, 21].

However, TiO_2 photocatalyst in the anatase phase has limited application under visible light irradiation due to its inherent high band gap energy (3.2 eV) [22]. In order to overcome this limitation, many efforts have been made to enable its visible light response by doping with transition metals (Ag, Cd, Cu) or non-metallic elements (C, S, N) [23, 24, 25]. Among these, nitrogen is the most preferred anionic dopant because of its ability to modify the electronic structure of TiO_2 by forming a new N 2p band above the O 2p valence band [26, 27]. This modification narrower the TiO_2 band gap and eventually shifts the optical absorption of this photocatalyst to the visible light spectrum [28].

In this work, we report the green synthesis of N-doped TiO_2 through the biosynthesis method using *Aloe vera* (L.) Burm f. as a natural capping agent, combined with a nitrogen doping process through the hydrothermal method for photocatalytic reduction of Cr(VI) under visible light irradiation. The effects of various ammonia concentrations on the characteristic and ability of this synthesized photocatalyst on the photocatalytic reduction of Cr(VI) were investigated.

2. Experiments

2.1. Materials and Tools

The materials used in this study were $TiCl_4$ (Merck), *Aloe vera* (L.) Burm. f. rind extract, ammonia 25% (Merck), ethanol (analytical grade, Merck), potassium dichromate ($K_2Cr_2O_7$, Merck), distilled water, H_2SO_4 (analytical grade, Merck), 1,5-diphenylcarbazide (Merck). All chemicals were used as received. Glassware, magnetic stirrer, Whatman filter paper, oven, analytical balance, centrifuge, pH meter, hot plate, and light source (24-watt yellow LED lamp, VISALUX) were used in the research. The instruments used were UV-Vis Spectrophotometer (Genesys 20), UV-Vis DRS (SPEC ORD 210 Plus), SEM-EDX (SEM SU3500, XRD (XPERT PRO PANalytical PW 30/40), and GSA (Quantachrome Nova 4200e).

2.2. Preparation of *Aloe vera* (L) Burm f. Extract

Aloe vera (L) Burm f. leaf samples were removed and separated from the gel, which was thoroughly washed and crushed. Then, 10 g of the samples were boiled in 100 mL of deionized water for 1 hour at 70°C. Leaf extract was filtered using Whatman filter paper.

2.3. Biosynthesis of TiO_2 Nanoparticles

A solution of titanium chloride (1 M, $TiCl_4$) was prepared in 100 mL of deionized water. Then 0.5 mL of the leaf extract was added dropwise under constant stirring (pH~7). The nanoparticles formed during the process were collected by centrifugation (10,000 rpm) and repeatedly washed with ethanol. The nanoparticles were rewashed with distilled water and dried at 100°C for 10 hours for further characterization.

2.4. Preparation of N-doped TiO_2 Powder

Briefly, 5 mL of 1 M $TiCl_4$ solution was placed into the flask under vigorous magnetic stirring in a closed state. After that, 50 mL of deionized water was added, followed by 0.5 mL of *Aloe vera* (L.) Burm f. leaf extract dropwise under continuous stirring. Then, 1 M NaOH was added until pH 7 and vigorously stirred for 24 hours. The formed nanoparticles were separated using centrifugation and then continuously washed using ethanol and distilled water to remove impurities. The obtained precipitate was dried at 100°C for 10 hours and calcined at 500°C for 1 hour to form TiO_2 powder.

Herein, the obtained TiO_2 powder was doped with nitrogen through hydrothermal. Respectively, 0.05 g of TiO_2, 12 mL of ethanol, 8 mL of deionized water, and 10% w/w ammonia (as N source) were added into a 50 mL vessel cylinder. This mixture was stirred for 2 hours and then heated at 180°C for 12 hours in an autoclave. After that, the obtained precipitate was filtered and washed with distilled water. Finally, it was dried at 105°C for 12 hours and calcined at 500°C for 1 hour. The resulting product was labeled as NTO10. The same steps were repeated for variations in the addition of NH_4OH 20% w/w, 35% w/w, and 50% w/w, labeled as NTO20, NTO35, and NTO50, respectively. The synthesis of N-doped TiO_2 without additional NH_4OH (labeled as TO) was used as a control.

2.5. Characterization of N-doped TiO_2 Nanoparticles

The samples of N-doped TiO_2 nanoparticles were characterized using X-ray Diffraction (XRD) to observe the crystalline phase and Diffuse Reflectance Spectra UV-Vis (DRS UV-Vis) to investigate the optical properties. The surface morphology and composition of the samples were analyzed using scanning electron microscopy-energy dispersive X-ray (SEM-EDX). Brunauer-Emmett-Teller (BET) method was employed to determine the specific surface area, pore diameter, and pore volume.

2.6. Photocatalytic Activity Test of N-doped TiO_2 Nanoparticles

TiO_2 nanoparticles of as much as 0.05 g were added to a solution containing 100 mL of Cr (VI) with a 10 mg/L concentration. A 6 N H_2SO_4 was added to the solution until

pH 2. The solution was stirred for 30 minutes in the dark. The solution was divided into ten test tubes, and each test tube contained 10 mL of solution. Then five test tubes were irradiated under a 24-watt LED light, and the other five test tubes were carried out in the dark for 120 minutes each. A total of 10 mL of the solution was taken every 30 minutes and centrifuged. The absorbance was determined using a UV-Vis spectrophotometer at 543 nm, and the dye used was 1,5-diphenylcarbazide 0.5%.

3. Results and Discussion

Photocatalyst N-doped TiO_2 was synthesized through a combination of the biosynthesis method using *Aloe vera* (L.) Burmf. as a capping agent in TiO_2 preparation, followed by the hydrothermal method on the nitrogen doping process. All synthesized photocatalysts were obtained in powder form and were yellowish-white in color. This is different when compared to pure TiO_2, which is pure white. This color change was caused by modifying the TiO_2 band gap by nitrogen doping, which shifts the optical absorption of this photocatalyst [22]. A detailed explanation of this information will be discussed in the optical properties section supported by UV-Vis spectroscopy analysis.

3.1. X-ray Diffraction (XRD)

The crystalline phase of the synthesized TiO_2 photocatalyst was determined using XRD. Figure 1(a-d) shows the typical XRD pattern of all synthesized photocatalyst samples. Respectively, the XRD peaks at 2θ = 25.3, 37.87, 48.05, 53.93, 55.10, and 62.79 can be assigned to (101), (004), (200), (105), and (211) crystal planes, which are often taken as the characteristic peaks of anatase TiO_2 (ICSD No.9855). No peaks of brookite or rutile were detected, indicating the high purity of these synthesized photocatalysts.
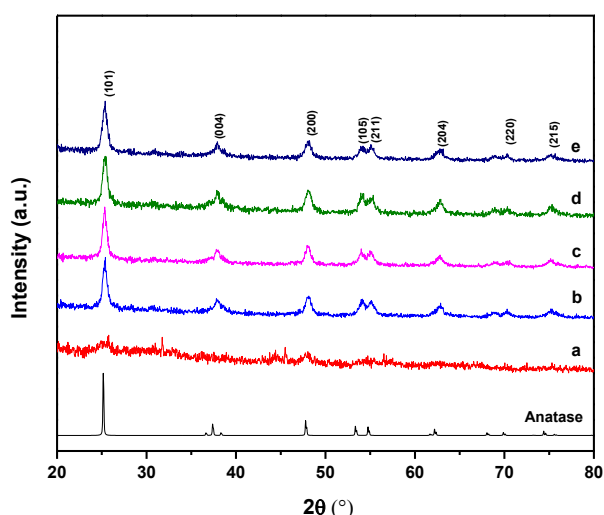

Figure 1. XRD diffraction patterns of a) TO, b) NTO10, c) NTO20, d) NTO35, and e) NTO50

3.2. The Optical Properties

The optical characterization of the synthesized photocatalyst was determined using UV-Vis DRS. As shown in Figure 2 (a-e), the samples of NTO10, NTO20, NTO35, and NTO50 show increased absorption in the visible region, especially at 400-550 nm compared to the undoped TiO_2 (TO sample). It is confirmed that since the undoped TiO_2 has a strong absorption on the UV light, it appears in pure white color. In contrast, shifting absorption to the visible region caused all the synthesized N-doped TiO_2 to appear yellowish [22].
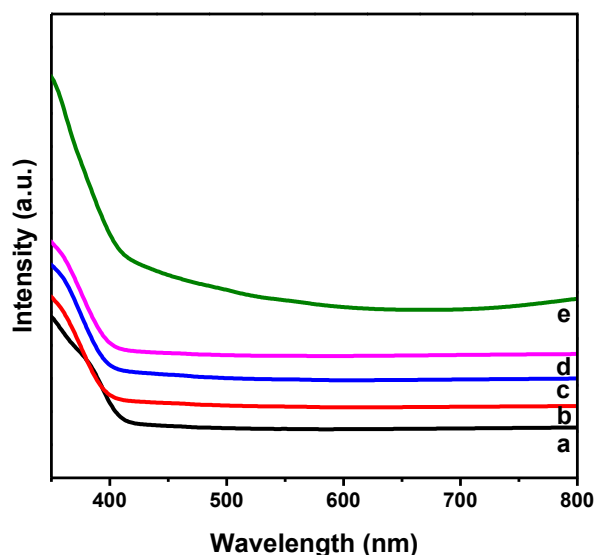

Figure 2. UV-Vis diffuse reflectance spectra of a) TO, b) NTO10, c) NTO20, d) NTO35, and e) NTO50

Figure 3 shows the relationship between the absorption coefficient and the absorbed energy/photon (hv). The X-axis shows the absorbed energy/photon (hv) value as an independent variable. The Y-axis shows the product of the absorption coefficient with energy $(\alpha hv)^2$ as the dependent variable. Using the Tauc plot method, the band gap of the photocatalyst can be determined by drawing a straight line between the outcome of the absorption coefficient [29].

By applying the Tauc plot method, the band gap energies for all of the synthesized photocatalysts can be calculated. Figure 3 shows the band gap of all as-prepared N-doped TiO_2, which is lower than the intrinsic band gap of anatase TiO_2 (3.2 eV). The decrease in the band gap proves that nitrogen has been successfully doped into TiO_2 nanoparticles. It is found that nitrogen doping reduced the band gap energy of the synthesized photocatalysts by forming a new N 2p band between the O 2p and Ti 3d valence band in the TiO_2 electronic structure [22, 26]. Due to the low band gap energy, the synthesized photocatalyst can trigger electron migration from the valence band to the conduction band by absorbing energy from the visible light region [27, 28].
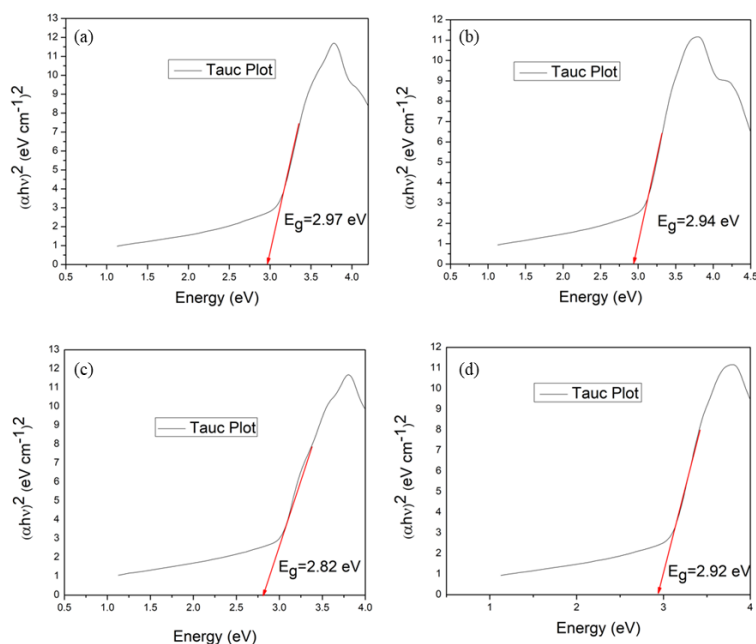
Figure 3. Graph of the energy gap (Eg) determination of a) NTO10, b) NTO20, c) NTO35, and d) NTO50
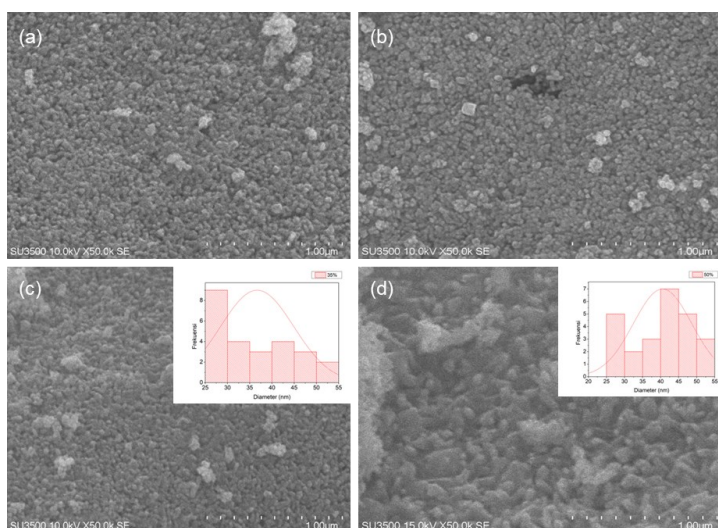

Figure 4. SEM images and distribution of N−doped TiO$_2$ nanoparticles: (a) NTO10, (b) NTO20, (c) NTO35, and (d) NTO50

As shown in Figure 3(b-c), the band gap energies of NTO10, NTO20, and NTO35 tend to decrease as nitrogen concentration increases. However, the band gap energy of NTO50 shows a slight increase compared to NTO35. It was found that nitrogen concentration with 35% w/w is an optimum N-doping level corresponding to high photoresponse for visible light. Here we assumed that at optimum nitrogen concentration, some localized N 2p states are formed above the valence band in N-doped anatase, leading band gap energy to narrow and thus inducing a red shift at the edge of the optical absorption range [30, 31]. As the nitrogen concentration increases beyond the optimum level, the localized N 2p states are mixed with the valence band, causing a slight increase in the band gap energy [32].

3.3. Scanning Electron Microscope-Electron Dispersive X-Ray (SEM-EDX)

SEM characterization was carried out to determine the surface morphology of the synthesized photocatalysts. Figure 4(a-d) shows the SEM images of all the synthesized N-doped TiO$_2$. It is apparently seen from Figure 4(a-c) that the particles of NTO10, NTO20, and NTO35 are homogeneous spherical with sizes from 15-55 nm. The effect of *Aloe vera* (L) Burm F. extracts as a natural capping agent is observed in controlling the agglomeration and reducing the particle size of N-doped TiO$_2$ [33]. The uniformity of the NTO35 particles, as shown in the particle size distribution graph (Figure 4c), implies that the biomolecule of *Aloe vera* (L) Burm F. extract have a good association with N-doped TiO$_2$ nanoparticles during the synthesis process [16]. However, Figure 4d shows the uneven particle size distribution of NTO50. Although the *Aloe vera* (L) Burm F. extract has been proven to prevent agglomeration during synthesis, high concentrations of nitrogen dopants can still cause nanoparticles to form aggregates [34].

Characterization of Energy Dispersive X-ray (EDX) aims to determine the elemental composition of the

synthesized photocatalyst. Figure 5 shows that NTO10, NTO20, NTO35, and NTO50 exhibit sharp and robust peaks in titanium (Ti), oxygen (O), and nitrogen (N). While the undoped TiO_2 (TO) only showed titanium (Ti)

and Oxygen (O) peaks. The appearance of the N element showed that N-doped TiO_2 nanoparticles had been successfully carried out by adding NH_4OH.
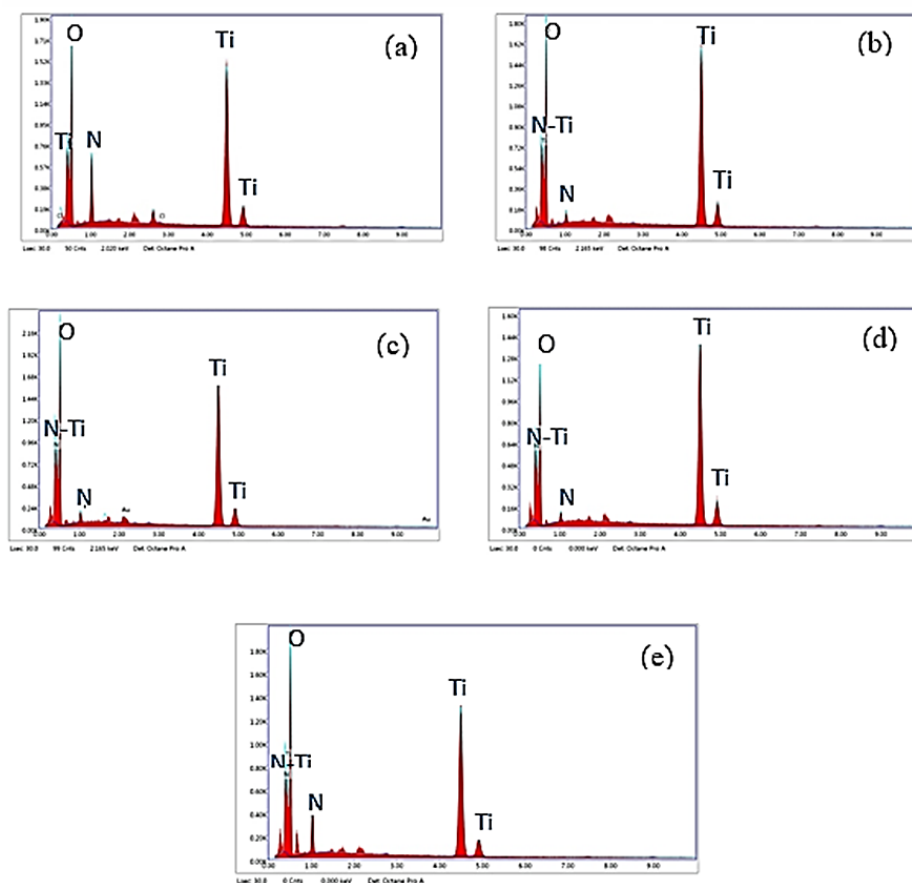

Figure 5. EDX spectrum of a) TO, b) NTO10, c) NTO20, d) NTO35, and e) NTO50

3.4. Surface Area Analysis

Surface area analysis determined the specific surface area, pore diameter, and pore volume of all synthesized photocatalysts. The results of the BET test can be seen in Figure 6. Based on Figure 6, the synthesized TiO_2 (TO) and 35% N-doped TiO2 (NTO35) samples have an isotherm curve IV, indicating that the sample is a mesoporous solid with multiple pore sizes ranging from 6-8 nm.
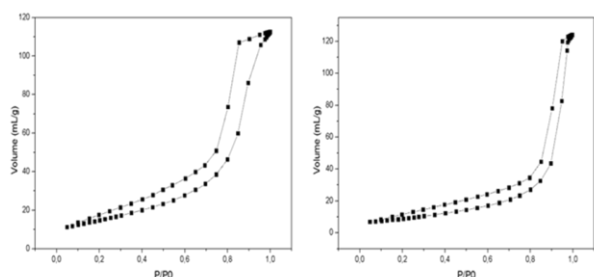

Figure 6. BET isotherm curves of (a) TO and (b) NTO35

The surface area of the photocatalyst is one of the essential parameters that can significantly affect photocatalytic activity. Table 1 presents the surface area, pore diameter, and pore volume using BET characterization. The surface area and pore diameter obtained in this study were 52.34 m²/g and 6.516 nm for TO and 31.81 m²/g; 1.47 nm for NTO35, respectively.

Table 1. Results of BET for specific surface area, pore diameter, and pore volume

No	Sample	Surface area (m²/g)	Pore diameter(nm)	Pore volume (mL/g)
1	TiO_2	52.34	6.516	0.174
2	N-doped TiO_2	31.81	1.47	0.190

3.5. Photocatalytic Activity Test

The photocatalytic activity test was carried out to see the ability of the photocatalyst to reduce metal ions. In this study, the metal ion used is Cr (VI), which will be reduced to Cr (III) with a concentration of 10 mg/L under a 24-watt LED lamp irradiation. Cr(VI) solution was added with 1,5-diphenylcarbazide complexing with a concentration of 0.5% to produce a purplish-colored chelate complex40. The complex reaction can be seen in Figure 7. Figure 8 shows the photoreduction ratio of Cr(VI) with all the synthesized photocatalysts under 120 minutes of visible light irradiation.
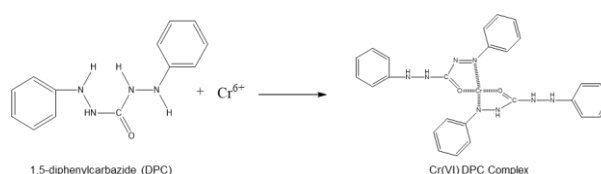

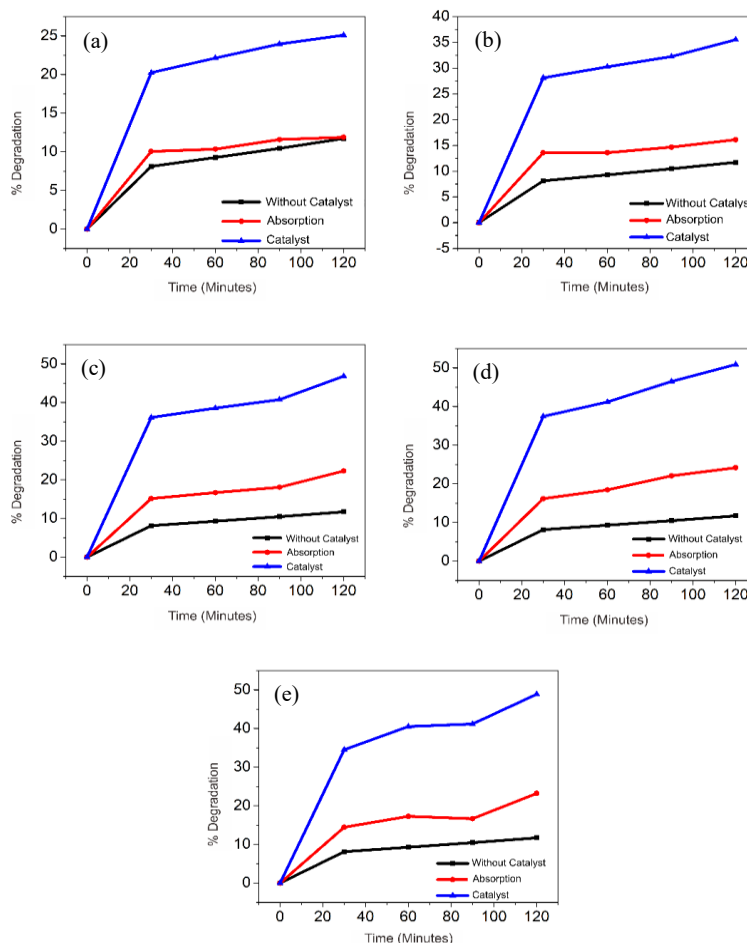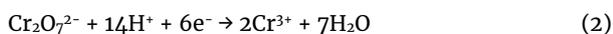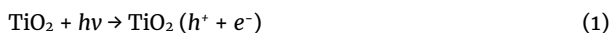**Figure 7**. Reaction of Cr (VI)-DPC complex formation

Figure 8. Reduction percentage of metal ions Cr (VI) at time variation of 0 to 120 minutes by a) TO, b) NTO10, c) NTO20, d) NTO35, e) NTO50 (blue= % total photoreduction (photocatalyst effect + absorption), red = % absorption of catalyst, black = % photoreduction of negative control)

Figure 8 shows that the photocatalyst and the absorption factor influence the reduction percentage of Cr (VI) ions. The reduction percentage increases as the irradiation time increases, leading to extending the photocatalytic reaction to reduce Cr (VI) to Cr (III). The reaction can be seen as follow:

$$TiO_2 + h\nu \rightarrow TiO_2\ (h^+ + e^-) \tag{1}$$

$$Cr_2O_7{}^{2-} + 14H^+ + 6e^- \rightarrow 2Cr^{3+} + 7H_2O \tag{2}$$

$$2H_2O + 4h^+ \rightarrow O_2 + 4H^+ \tag{3}$$

The photocatalytic mechanism of Cr(VI) to Cr(III) reduction in nano-sized N-doped TiO₂ is illustrated in Figure 9. When N-doped TiO₂ is exposed to photons (light) with energy equal to or greater than the band gap energy, electrons in the valence band will be excited to the conduction band, causing the photocatalytic process to occur. Electrons (e⁻) that are excited to the valence band will react with metal ions Cr (VI) to produce metal ions Cr (III). The results of the photoreduction test for Cr (VI) metal ions with all the synthesized photocatalysts under 120 minutes irradiation are shown in Figure 10.
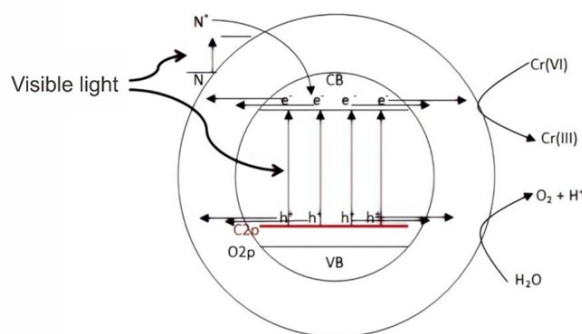

Figure 9. Mechanism of photoreduction of metal ion Cr (VI) to Cr (III)

Figure 10 shows that the synthesized N-doped TiO₂ with a nitrogen concentration of 35% w/w (NTO35) showed the highest photoreduction activity of 50.88% compared to other samples. Figure 10 shows that the highest photoreduction percentage of Cr(VI) was successfully accomplished by synthesized N-doped TiO₂ with a nitrogen concentration of 35% w/w (NTO35) under 120 minutes visible light irradiation. Approximately 50.88% of Cr(VI) was reduced from the aqueous solutions in the presence of this photocatalyst. Meanwhile, only 25.1%, 34.51%, 46.8%, and 48.89% of Cr(VI) were reduced by TO, NTO10, NTO20, and NTO50, respectively.
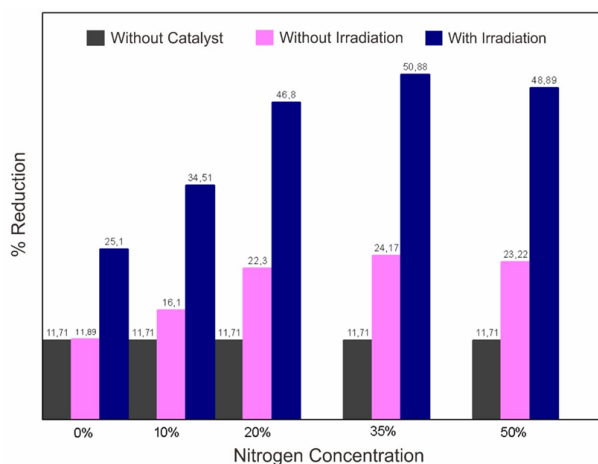
Figure 10. Bar chart of reduction percentage of metal ions Cr (VI) at time variation of 0 to 120 minutes by a) TO, b) NTO10, c) NTO20, d) NTO35, e) NTO50 (blue= % total photoreduction (photocatalyst effect + absorption), red = % absorption of catalyst, black = % photoreduction of negative control)

Here, the surface area, anatase fraction, and nitrogen doping were found to be the most important factors governing photocatalytic activity [22, 26]. Therefore, the obtained results indicated that synthesized N-doped TiO$_2$ photocatalyst using *Aloe vera* (L) Burm f. extract with the optimum nitrogen dopant concentration exhibited higher activity than other photocatalyst samples due to its higher specific surface area, a higher fraction of active anatase phase and higher absorption in the visible light region [35].

4. Conclusion

In summary, N-doped TiO$_2$ photocatalysts were successfully synthesized by combining biosynthesis and hydrothermal methods using *Aloe vera* (L) Burm F. extract as a natural capping agent. The nitrogen concentration of 35% w/w was suggested as the optimum dopant concentration to prepare N-doped TiO$_2$. Using synthesized NTO35 photocatalyst, about 50.88% of Cr(VI) could be reduced under 120 minutes visible light irradiation. The enhanced photocatalytic activity on the photoreduction of Cr(VI) was mainly attributed to the association of *Aloe vera* (L.) Burm F. extract in preventing the agglomeration and increasing the surface area during the TiO$_2$ synthesis process, as well as the influence of N-dopant in enhancing the anatase fraction and narrowing the band gap energy.

Acknowledgment

References

[1] Jessica Briffa, Emmanuel Sinagra, Renald Blundell, Heavy metal pollution in the environment and their toxicological effects on humans, *Heliyon*, 6, 9, (2020), e04691 https://doi.org/10.1016/j.heliyon.2020.e04691

[2] Marzieh Mokarram, Ali Saber, Vahideh Sheykhi, Effects of heavy metal contamination on river water quality due to release of industrial effluents, *Journal of Cleaner Production*, 277, (2020), 123380 https://doi.org/10.1016/j.jclepro.2020.123380

[3] Md Nur-E-Alam, Md Abu Sayid Mia, Farid Ahmad, Md Mafizur Rahman, An overview of chromium removal techniques from tannery effluent, *Applied Water Science*, 10, 9, (2020), 205 https://doi.org/10.1007/s13201-020-01286-0

[4] Annamalai Raja, Palani Rajasekaran, Karuppaiah Selvakumar, Mukannan Arivanandhan, Sultan Asath Bahadur, Meenakshisundaram Swaminathan, Efficient photoreduction of hexavalent chromium using the reduced graphene oxide−Sm$_2$MoO$_6$−TiO$_2$ catalyst under visible light illumination, *ACS Omega*, 5, 12, (2020), 6414-6422 https://doi.org/10.1021/acsomega.9b03923

[5] Rakesh Shrestha, Sagar Ban, Sijan Devkota, Sudip Sharma, Rajendra Joshi, Arjun Prasad Tiwari, Hak Yong Kim, Mahesh Kumar Joshi, Technological trends in heavy metals removal from industrial wastewater: A review, *Journal of Environmental Chemical Engineering*, 9, 4, (2021), 105688 https://doi.org/10.1016/j.jece.2021.105688

[6] Lu Xu, Xue Bai, Linkai Guo, Shengjiong Yang, Pengkang Jin, Lei Yang, Facial fabrication of carbon quantum dots (CDs)-modified N-TiO$_{2-x}$ nanocomposite for the efficient photoreduction of Cr(VI) under visible light, *Chemical Engineering Journal*, 357, (2019), 473-486 https://doi.org/10.1016/j.cej.2018.09.172

[7] Ying Zhao, Donglin Zhao, Changlun Chen, Xiangke Wang, Enhanced photo-reduction and removal of Cr(VI) on reduced graphene oxide decorated with TiO$_2$ nanoparticles, *Journal of Colloid and Interface Science*, 405, (2013), 211-217 https://doi.org/10.1016/j.jcis.2013.05.004

[8] Jianhao Qiu, Ming Li, Lvye Yang, Jianfeng Yao, Facile construction of three-dimensional netted ZnIn$_2$S$_4$ by cellulose nanofibrils for efficiently photocatalytic reduction of Cr(VI), *Chemical Engineering Journal*, 375, (2019), 121990 https://doi.org/10.1016/j.cej.2019.121990

[9] Ting Ge, Zhikang Jiang, Li Shen, Jing Li, Zhiqi Lu, Yongcai Zhang, Fang Wang, Synthesis and application of Fe$_3$O$_4$/FeWO$_4$ composite as an efficient and magnetically recoverable visible light-driven photocatalyst for the reduction of Cr(VI), *Separation and Purification Technology*, 263, (2021), 118401 https://doi.org/10.1016/j.seppur.2021.118401

[10] Pooja Sharma, Surendra Pratap Singh, Sheetal Kishor Parakh, Yen Wah Tong, Health hazards of hexavalent chromium (Cr (VI)) and its microbial reduction, *Bioengineered*, 13, 3, (2022), 4923-4938 https://doi.org/10.1080/21655979.2022.2037273

[11] Anh Binh Ngo, Hong Lien Nguyen, Dirk Hollmann, Criticial assessment of the photocatalytic reduction of Cr(VI) over Au/TiO$_2$, *Catalysts*, 8, 12, (2018), 606 https://doi.org/10.3390/catal8120606

[12] Lingyi Zheng, Zhenglin Chen, Jingsong Han, Zhihui Wei, Lixia Yang, Mingxia Lu, Tianzhu Ma, Liming Yang, An all-in-one photocatalyst: Photocatalytic reduction of Cr(VI) and anchored adsorption of Cr(III) over mesoporous titanium@sulfonated

carbon hollow hemispheres, *Journal of Environmental Chemical Engineering*, 10, 3, (2022), 107864 https://doi.org/10.1016/j.jece.2022.107864

[13] Jayaseelan Arun, S. Nachiappan, Goutham Rangarajan, Ram Prasath Alagappan, K. P. Gopinath, Eric Lichtfouse, Synthesis and application of titanium dioxide photocatalysis for energy, decontamination and viral disinfection: A review, *Environmental Chemistry Letters*, 21, 1, (2023), 339-362 https://doi.org/10.1007/s10311-022-01503-z

[14] Shipra Mital Gupta, Manoj Tripathi, A review on the synthesis of TiO₂ nanoparticles by solution route, *Central European Journal of Chemistry*, 10, 2, (2012), 279-294 https://doi.org/10.2478/s11532-011-0155-y

[15] Muhammad Atif Irshad, Rab Nawaz, Muhammad Zia ur Rehman, Muhammad Adrees, Muhammad Rizwan, Shafaqat Ali, Sajjad Ahmad, Sehar Tasleem, Synthesis, characterization and advanced sustainable applications of titanium dioxide nanoparticles: A review, *Ecotoxicology and Environmental Safety*, 212, (2021), 111978 https://doi.org/10.1016/j.ecoenv.2021.111978

[16] Syamsutajri Syamsol Bahri, Zawati Harun, Siti Khadijah Hubadillah, Wan Norhayati Wan Salleh, Nurafiqah Rosman, Noor Hasliza Kamaruddin, Faiz Hafeez Azhar, Norsuhailizah Sazali, Raja Adiba Raja Ahmad, Hatijah Basri, Review on recent advance biosynthesis of TiO₂ nanoparticles from plant-mediated materials: characterization, mechanism and application, *IOP Conference Series: Materials Science and Engineering*, 2021 https://doi.org/10.1088/1757-899X/1142/1/012005

[17] Meghmala S. Waghmode, Aparna B. Gunjal, Javed A. Mulla, Neha N. Patil, Neelu N. Nawani, Studies on the titanium dioxide nanoparticles: Biosynthesis, applications and remediation, *SN Applied Sciences*, 1, 4, (2019), 310 https://doi.org/10.1007/s42452-019-0337-3

[18] Agnes Mbonyiryivuze, Sidiki Zongo, Abdoulaye Diallo, Sone Bertrand, Evariste Minani, Lakhan Lal Yadav, Bonex W. Mwakikunga, Simon Mokhotjwa Dhlamini, Malik Maaza, Titanium dioxide nanoparticles biosynthesis for dye sensitized solar cells application: review, *Physics and Materials Chemistry*, 3, 1, (2015), 12-17

[19] Brian Yuliarto, Ni Luh Wulan Septiani, Yusuf Valentino Kaneti, Muhammad Iqbal, Gilang Gumilar, Minjun Kim, Jongbeom Na, Kevin C.-W. Wu, Yusuke Yamauchi, Green synthesis of metal oxide nanostructures using naturally occurring compounds for energy, environmental, and bio-related applications, *New Journal of Chemistry*, 43, 40, (2019), 15846-15856 https://doi.org/10.1039/C9NJ03311D

[20] F. E. Ettadili, S. Aghris, F. Laghrib, A. Farahi, S. Saqrane, M. Bakasse, S. Lahrich, M. A. El Mhammedi, Recent advances in the nanoparticles synthesis using plant extract: Applications and future recommendations, *Journal of Molecular Structure*, 1248, (2022), 131538 https://doi.org/10.1016/j.molstruc.2021.131538

[21] Mohammad Aslam, Ahmad Zuhairi Abdullah, Mohd Rafatullah, Recent development in the green synthesis of titanium dioxide nanoparticles using plant-based biomolecules for environmental and antimicrobial applications, *Journal of Industrial and Engineering Chemistry*, 98, (2021), 1-16 https://doi.org/10.1016/j.jiec.2021.04.010

[22] Diana Vanda Wellia, Dina Nofebriani, Nurul Pratiwi, Safni Safni, Synthesis of Porous N-doped TiO₂ by Using Peroxo Sol-Gel Method for Photocatalytic Reduction of Cd(II), *Bulletin of Chemical Reaction Engineering & Catalysis*, 17, 1, (2022), 103-112 https://doi.org/10.9767/bcrec.17.1.12347.103-112

[23] Patil S. Basavarajappa, Shivaraj B. Patil, Nagaraju Ganganagappa, Kakarla Raghava Reddy, Anjanapura V. Raghu, Ch. Venkata Reddy, Recent progress in metal-doped TiO₂, non-metal doped/codoped TiO₂ and TiO₂ nanostructured hybrids for enhanced photocatalysis, *International Journal of Hydrogen Energy*, 45, 13, (2020), 7764-7778 https://doi.org/10.1016/j.ijhydene.2019.07.241

[24] Anna Khlyustova, Nikolay Sirotkin, Tatiana Kusova, Anton Kraev, Valery Titov, Alexander Agafonov, Doped TiO₂: The effect of doping elements on photocatalytic activity, *Materials Advances*, 1, 5, (2020), 1193-1201 https://doi.org/10.1039/D0MA00171F

[25] Jong‐Pil Jeon, Do Hyung Kweon, Boo Jae Jang, Myung Jong Ju, Jong‐Beom Baek, Enhancing the photocatalytic activity of TiO₂ catalysts, *Advanced Sustainable Systems*, 4, 12, (2020), 2000197 https://doi.org/10.1002/adsu.202000197

[26] Shiwen Du, Juhong Lian, Fuxiang Zhang, Visible light-responsive N-doped TiO₂ photocatalysis: Synthesis, characterizations, and applications, *Transactions of Tianjin University*, 28, (2021), 33−52 https://doi.org/10.1007/s12209-021-00303-w

[27] Shu Qin Wang, Wen Bo Liu, Peng Fu, Wei Liang Cheng, Enhanced photoactivity of N-doped TiO₂ for Cr(VI) removal: Influencing factors and mechanism, *Korean Journal of Chemical Engineering*, 34, (2017), 1584-1590 https://doi.org/10.1007/s11814-017-0003-7

[28] Xiao Li, Pengwei Liu, Yu Mao, Mingyang Xing, Jinlong Zhang, Preparation of homogeneous nitrogen-doped mesoporous TiO₂ spheres with enhanced visible-light photocatalysis, *Applied Catalysis B: Environmental*, 164, (2015), 352-359 https://doi.org/10.1016/j.apcatb.2014.09.053

[29] Peverga R. Jubu, O. S. Obaseki, A. Nathan-Abutu, F. K. Yam, Yushamdan Yusof, M. B. Ochang, Dispensability of the conventional Tauc's plot for accurate bandgap determination from UV−vis optical diffuse reflectance data, *Results in Optics*, 9, (2022), 100273 https://doi.org/10.1016/j.rio.2022.100273

[30] Hsuan-Chung Wu, Syuan-Wei Lin, Jhao-Sian Wu, Effects of nitrogen concentration on N-doped anatase TiO₂: density functional theory and Hubbard *U* analysis, *Journal of Alloys and Compounds*, 522, (2012), 46-50 https://doi.org/10.1016/j.jallcom.2012.01.071

[31] Hsyi-En Cheng, Yu-Ru Chen, Wen-Tuan Wu, Ching-Ming Hsu, Effect of nitrogen doping concentration on the properties of TiO₂ films grown by atomic layer deposition, *Materials Science and Engineering: B*, 176, 7, (2011), 596-599 https://doi.org/10.1016/j.mseb.2011.02.001

[32] Kesong Yang, Ying Dai, Baibiao Huang, Study of the nitrogen concentration influence on N-doped TiO_2 anatase from first-principles calculations, *The Journal of Physical Chemistry C*, 111, 32, (2007), 12086−12090 https://doi.org/10.1021/jp067491f

[33] K. S. Venkatesh, S. R. Krishnamoorthi, N. S. Palani, V. Thirumal, Sujin P. Jose, Fu-Ming Wang, R. Ilangovan, Facile one step synthesis of novel TiO_2 nanocoral by sol−gel method using *Aloe vera* plant extract, *Indian Journal of Physics*, 89, (2015), 445−452 https://doi.org/10.1007/s12648-014-0601-8

[34] Tao Xu, Mo Wang, Tong Wang, Effects of N doping on the microstructures and optical properties of TiO_2, *Journal Wuhan University of Technology, Materials Science Edition*, 34, 1, (2019), 55−63 https://doi.org/10.1007/s11595-019-2014-1

[35] S. Srujana, M. Anjamma, Bharat Singh, Ram C. Dhakar, Shanthi Natarajan, Ramana Hechhu, A Comprehensive Study on the Synthesis and Characterization of TiO_2 Nanoparticles Using Aloe vera Plant Extract and Their Photocatalytic Activity against MB Dye, *Adsorption Science & Technology*, 2022, (2022), 7244006 https://doi.org/10.1155/2022/7244006